AMERICAN SOCIETY FOR MICROBIOLOGY | Antimicrobial Agents and Chemotherapy®

ANTIVIRAL AGENTS

Population Pharmacokinetic Model Linking Plasma and Peripheral Blood Mononuclear Cell Concentrations of Efavirenz and Its Metabolite, 8-Hydroxy-Efavirenz, in HIV Patients

Abiy Habtewold,[a] Eleni Aklillu,[b] Eyasu Makonnen,[c] Getnet Yimer,[c] Leif Bertilsson,[b] Jürgen Burhenne,[d] Joel S. Owen[a]

Department of Pharmaceutical Sciences, School of Pharmacy, Union University, Jackson, Tennessee, USA[a]; Division of Clinical Pharmacology, Department of Laboratory Medicine, Karolinska University Hospital Huddinge, Karolinska Institutet, Stockholm, Sweden[b]; Department of Pharmacology, School of Medicine, Addis Ababa University, Addis Ababa, Ethiopia[c]; Department of Clinical Pharmacology and Pharmacoepidemiology, University of Heidelberg, Heidelberg, Germany[d]

ABSTRACT The objectives of this study were to characterize the population pharmacokinetics (PK) of efavirenz (EFV) and 8-hydroxy-efavirenz (8OHEFV) in plasma and peripheral blood mononuclear cells (PBMCs) and to explore covariates affecting the PK parameters. Fifty-one patients had steady-state 0-to-24-h concentrations of EFV and 8OHEFV in plasma with corresponding concentrations in PBMCs, while 261 patients had one or two sparse concentrations at 16 ± 1 h postdose at weeks 4 and/or 16. The pharmacogenetic markers *CYP2B6*6*, *CYP3A5*3*, *CYP3A5*6*, *UGT2B7*2*, *ABCB1* (3435C→T, 3842A→G), *OATP1B1*1B*, and *OATP1B1*5*, the presence of a rifampin-based antituberculosis (anti-TB) regimen, baseline body weight and organ function values, and demographic factors were explored as covariates. EFV concentration data were well described by a two-compartment model with first-order absorption (K_a) and absorption lag time (A_{lag}) (K_a = 0.2 h^{-1}; A_{lag} = 0.83 h; central compartment clearance [CL_c/F] for *CYP2B6*1/*1* = 18 liters/h, for *CYP2B6*1/*6* = 14 liters/h, and for *CYP2B6*6/*6* = 8.6 liters/h) and PBMCs as a peripheral compartment. EFV transfer from plasma to PBMCs was first order (CL_p/F = 32 liters/h), followed by capacity-limited return (V_{max} = 4,400 ng/ml/h; K_m = 710 ng/ml). Similarly, 8OHEFV displayed a first-order elimination and distribution to PBMCs, with a capacity-limited return to plasma. No covariate relationships resulted in a significant explanation of interindividual variability (IIV) on the estimated PK parameters of EFV and 8OHEFV, except for *CYP2B6*6* genotypes, which were consistent with prior evidence. Both EFV and 8OHEFV accumulated to higher concentrations in PBMCs than in plasma and were well described by first-order input and Michaelis-Menten kinetics removal from PBMCs. *CYP2B6*6* genotype polymorphisms were associated with decreased EFV and 8OHEFV clearance.

KEYWORDS efavirenz, 8-hydroxy-efavirenz, peripheral blood mononuclear cells, population pharmacokinetics

Received 31 January 2017 **Returned for modification** 14 March 2017 **Accepted** 21 May 2017

Accepted manuscript posted online 30 May 2017

Citation Habtewold A, Aklillu E, Makonnen E, Yimer G, Bertilsson L, Burhenne J, Owen JS. 2017. Population pharmacokinetic model linking plasma and peripheral blood mononuclear cell concentrations of efavirenz and its metabolite, 8-hydroxy-efavirenz, in HIV patients. Antimicrob Agents Chemother 61:e00207-17. https://doi.org/10.1128/AAC.00207-17.

Address correspondence to Abiy Habtewold, abiyeyakem@gmail.com.

Efavirenz (EFV)-based antiretroviral therapy remains the preferred first-line treatment option in important international guidelines, including those of the World Health Organization (1). EFV displays a wide between-patient pharmacokinetic (PK) variability (2, 3). This is ascribed partially to genetic variation of the CYP2B6 enzyme, which is primarily responsible for the metabolism of efavirenz to 8-hydroxy-efavirenz (8OHEFV) (4, 5). Efavirenz is described to have a narrow safety margin (6–8). In addition, a couple

of recent reports in part incriminated 8OHEFV in the neurotoxic adverse reactions associated with efavirenz administration, emphasizing the need to characterize the time course of both EFV and 8OHEFV in the body (7, 9).

PK models describing the disposition of efavirenz in plasma have been reported previously (3, 10–13). A single study reported a PK model comprising both the parent drug (EFV) and the metabolite (8OHEFV) in plasma after a single dose that was lower than the recommended dose of efavirenz in 17 healthy Korean male subjects (14). This study in healthy volunteers does not represent the clinical scenario, given that treatment of HIV is lifelong, and the long-term administration of EFV with its complex autoinduction phenomenon is not addressed. HIV/AIDS patients display lower relative bioavailability of efavirenz than healthy subjects, and hence direct extrapolation of efavirenz exposure data from healthy volunteers to the target patient population may not be applicable (8). Moreover, since most antiretroviral drugs, including efavirenz, exert their therapeutic effects in the target immune cells (15), characterization of the intracellular time course of these drugs may result in the design of a more accurate and reliable dosage regimen. We are aware of no PK models that describe the time course of either EFV or 8OHEFV in plasma and intracellular compartments simultaneously.

Therefore, in the present study, we developed a population PK model to characterize the time course of EFV and 8OHEFV in plasma and peripheral blood mononuclear cells (PBMCs). We also evaluated covariates to explain the interindividual variability (IIV) of EFV and 8OHEFV pharmacokinetics. The explored covariates were demographic characteristics, baseline liver and renal function indices, and pharmacogenetic variables.

RESULTS

Characteristics of study subjects. A total of 1,185 EFV concentrations in plasma and in PBMCs ($n = 689$) and 1,091 8OHEFV concentrations in plasma and in PBMCs ($n = 310$) were included in the analysis. Table 1 summarizes the demographic characteristics with baseline organ function values and the distribution of pharmacogenetic determinants.

Pharmacokinetic model determination and parameter estimation. Concentration-time profiles and model comparisons suggested the presence of a peripheral compartment. Since EFV concentrations in PBMCs were measured in the present study, PBMCs were assumed to represent a peripheral compartment, and models with a nonspecific catenary or mammillary peripheral compartment were also tested. Simultaneous (combined) modeling was executed using the plasma and PBMC EFV concentration data. Since substantial accumulation occurred in the PBMCs, a nonlinear model with first-order transfer from the central to the peripheral compartment (CL_p EFV) and nonlinear return (V_{max} and K_m) was explored.

EFV data were well described by a two-compartment model with PBMC concentrations representing the peripheral compartment (Fig. 1). Three-compartment models, both as catenary and mammillary compartments, did not either converge successfully or converged at a higher objective function value (OFV) ($\Delta OFV > 700$ points) than that of other models. A proportional error model (constant coefficient of variation [CCV]) of residual variability performed better than the exponential, additive, and combined error models. The EFV absorption rate constant (K_a) and absorption lag time (A_{lag}) values were estimated from the full concentration-time profiles ($K_a = 0.2\ h^{-1}$, $A_{lag} = 0.83$ h) and fixed to these values in subsequent modeling steps that included the sparse concentration data. The estimated values of K_a and A_{lag} corroborated previous reports (10, 14).

EFV concentrations in PBMCs were substantially greater than simultaneous EFV concentrations in plasma. While EFV could be described using a first-order transfer kinetic process from the central to the peripheral (PBMC) compartment, its return was well described using a nonlinear saturable intercompartmental clearance process (Fig. 1). The population PK parameter estimates of EFV in plasma and PBMCs with IIV and residual error estimates are shown in Table 2. As outlined in Materials and Methods, the

TABLE 1 Patient characteristics[a]

Variable	Value[b]
Continuous	
Demography	
Age (yr)	34.0 (28.0–40.0)
Body wt (kg)	50.5 (46.0–56.0)
BMI (kg/m^2)	19.2 (17.5–21.0)
Baseline hematology	
Hemoglobin (g/dl)	12.3 (10.9–13.6)
Leukocyte (10^{9}cells/liter)	4.7 (3.7–5.9)
Neutrophils (10^{9}cells/liter)	46.0 (4.0–61.0)
Thrombocytes (10^{9}cells/liter)	241.0 (182.0–312.5)
Albumin (g/liter)	3.9 (3.4–4.3)
Baseline liver function panel	
AST (U/liter)	34.0 (27.5–49.0)
ALT (U/liter)	28.0 (24.0–26.0)
ALP (U/liter)	111.0 (91.0–138.5)
Total bilirubin (μmol/liter)	0.45 (0.3–0.9)
Direct bilirubin (μmol/liter)	0.1 (0.1–0.13)
Baseline renal function panel	
Blood urea (mg/dl)	24.0 (19.0–30.0)
Serum creatinine (μmol/liter)	0.9 (0.7–1.0)
Baseline virology and immunology	
HIV RNA ($\log_{10}$ copies/ml)	5.2 (4.5–5.5)
CD4 cells/mm^3	101.0 (54.5–149.5)
Categorical	
Rifampin-based anti-TB regimen	
Yes	81
No	232
Sex	
Males	104
Females	209
HBsAg	
Yes	17
No	296
HCV	
Yes	6
No	307
*CYP2B6*6* (516G→T)	
GG	144
GT	134
TT	20
ABCB1 (3435C→T)	
CC	185
CT	99
TT	14
ABCB1 (3842A→T)	
AA	222
AG	73
GG	7
*CYP3A5*3* (6986A→G)	
AA	37
AG	140
GG	121
*CYP3A5*6* (14690G→A)	
GG	222
GA	69
AA	7
*UCT2B7*2* (372G→A)	
GG	74
GA	163
AA	65
*OATP1B1*1B* (388A→G)	
AA	45
AG	152
GG	105

(Continued on next page)

TABLE 1 (Continued)

Variable	Value[b]
*OATP1B1*5* (521T→C)	
TT	202
TC	82
CC	18

[a]BMI, body mass index; HIV RNA, RNA of human immunodeficiency virus; CD4, cluster of differentiation 4; HBsAg, hepatitis B surface antigen; HCV, hepatitis C virus; IQR, interquartile range; AST, aspartate aminotransferase; ALT, alanine aminotransferase; ALP, alkaline phosphatase.
[b]Values for continuous variables are medians (IQRs); values for categorical variables are *n*.

*CYP2B6*6* genotype was used as a modifier of clearance in the base model. Exclusion of this modifier caused a misfit of the model and an increase in OFV by 44 points from the best model. Therefore, *CYP2B6*6* genotype status was retained in the base model.

Covariate relationships of the CL/*F*, central volume of distribution (V_c/F), and V_{max} of EFV were explored using delta plots and were added to the base model in a univariate process. None of the covariates tested significantly reduced the OFV of any of the estimates. However, inclusion of interoccasion variability (IOV) with the CL/*F* of EFV significantly improved the fit (119-point reduction in OFV from the prior model). Therefore, IOV was carried on subsequent model development steps.

As with EFV (the parent), 8OHEFV (the metabolite) was well described by first-order distribution from the central compartment to the peripheral PBMC compartment with saturable return (Fig. 1). While central compartment clearance (CL_c/F of 8OHEFV) was estimated (Table 3), its apparent central volume of distribution (V_c/F of 8OHEFV) was fixed to a literature value of 10 liters due to structural nonidentifiability (14). Also, whereas K_m was estimated for the return of 8OHEFV from the peripheral (PBMCs) to the central compartment, the apparent peripheral volume of distribution (V_p/F of 8OHEFV) and V_{max} of 8OHEFV were fixed to the EFV estimates (Table 3). In an exploration of the effect of covariates on the estimated CL_c/F of 8OHEFV, tests of the covariates sex and *UGT2B7*2* genotypes showed reductions in the OFV with an α of 0.05, but the overall reductions in IIV were only 2.3 and 0.8%, respectively. Therefore, they were not retained in the final model. Inclusion of IOV in the CL_c/F of 8OHEFV significantly improved the model fit.

Model diagnostics and evaluations. Overall, goodness-of-fit plots show that the model describes the observed concentrations of EFV and 8OHEFV in plasma and PBMCs sufficiently. The left and right top panels in Fig. 2 depict even distributions around the line of identity for both the population and individual EFV concentration predictions in plasma versus the observed concentrations, respectively, although with substantial variability. The conditional weighted residuals (CWRES) are within an acceptable

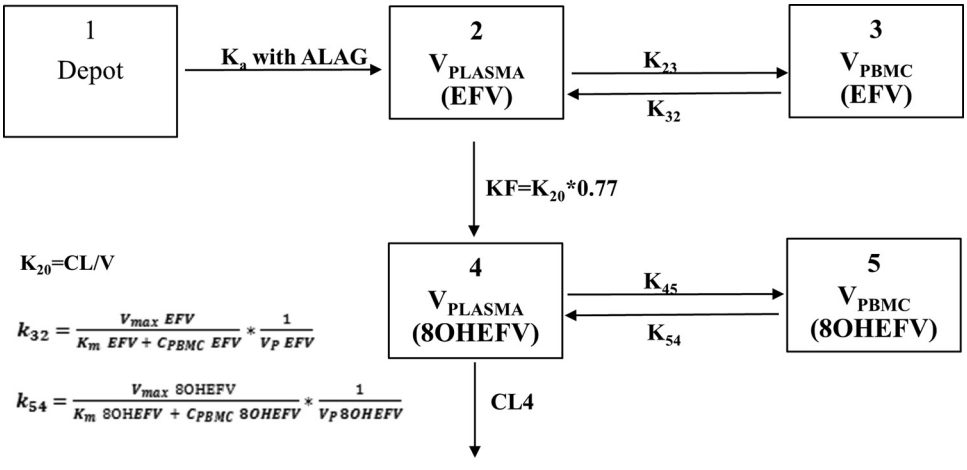

FIG 1 Structural pharmacokinetic model of EFV and 8OHEFV in plasma and PBMCs. ALAG, absorption lag time.

TABLE 2 Population PK parameter estimates of EFV in plasma and PBMCs[a]

Parameter	Final parameter estimate		IIV/residual variability	
	Typical value	%SEM	%CV	%SEM
K_a (1/h)	0.20[b]	NA	NE	NE
A_{lag}	0.83[b]	NA	NE	NA
V_c/F (liters), EFV in plasma	100	17	120	29
V_p/F (liters), EFV in PBMCs	210	87	NE	NA
V_{max} (ng/ml/h), EFV	4,400	72	50	17
K_m (ng/ml), EFV	710	74	NE	NA
CL_c/F (liters/h) for individuals with indicated genotype				
*CYP2B6*1/*1*	18	4.1	39	14
*CYP2B6*1/*6*	14	4.7	39	14
*CYP2B6*6/*6*	8.6	13	39	14
CL_p/F (liters/h) (central to PBMCs)	32[b]	7.8	NE	NE
RV in plasma	0.11[c]	8.5	34	NA
RV in PBMCs	0.42[c]	7.9	65	NA

[a]NA, not applicable; NE, not estimated; %CV, percentage of coefficient of variation; IIV, interindividual variability.
[b]Typical value fixed.
[c]Residual variance estimate.

range and are uniformly spread when CWRES are plotted versus time after dose and versus population predictions, as in the left and right bottom panels in Fig. 2. Although the concentrations of 8OHEFV in PBMCs appear to be evenly distributed around the line of identity, based on CWRES, high concentrations of 8OHEFV in plasma appear to be underpredicted. Figure 3 presents visual predictive check (VPC) plots of EFV and 8OHEFV in plasma and PBMCs at times of full-profile sample collections for 1,000 replicates using the final model, with observed data overlaid. Most of the EFV and 8OHEFV concentrations in plasma and PBMCs fall within the 5th and 95th percentiles. The median, 5th, and 95th percentile lines of the observed and predicted EFV and 8OHEFV concentrations in plasma and PBMCs are comparable, but a few outlying observations led to some differences in the 95th percentile lines.

DISCUSSION

In the present study, for the first time to the best of our knowledge, we characterize and report the population pharmacokinetics of efavirenz and its major metabolite, 8-hydyoxy-efavirenz, not only in plasma but also in peripheral blood mononuclear cells

TABLE 3 Population PK parameter estimates of 8OHEFV in plasma and PBMCs[a]

Parameter	Final parameter estimate		IIV/residual variability	
	Typical value	%SEM	%CV	%SEM
V_c/F (liters), 8OHEFV in plasma	10.00[b]	NA	NE	NA
CL_c/F (liters/h), 8OHEFV in plasma	185.5	4.37	60.26	4.1232
RV in plasma	0.2288[c]	7.64	47.83	NA
V_p/F (liters), 8OHEFV in PBMCs	210.0[b]	NA	NE	NA
CL_p/F (liters/h), 8OHEFV in PBMCs	216.1	23.15	NE	NA
V_{max} (ng/ml/h), 8OHEFV	4,400[b]	NA	NE	NA
K_m (ng/ml), 8OHEFV	37.11	22.96	94.76	10.88
RV in PBMC	0.3134[c]	11.76	55.99	NA

[a]Individual subject EFV model parameters were fixed for the estimation of 8OHEFV parameters in plasma. Individual subject parameters for EFV and 8OHEFV in plasma were fixed for the estimation of 8OHEFV in PBMCs. NA, not applicable; %CV, percentage of coefficient of variation; IIV, interindividual variability; NE, not estimated.
[b]Typical value fixed.
[c]Residual variance estimate.

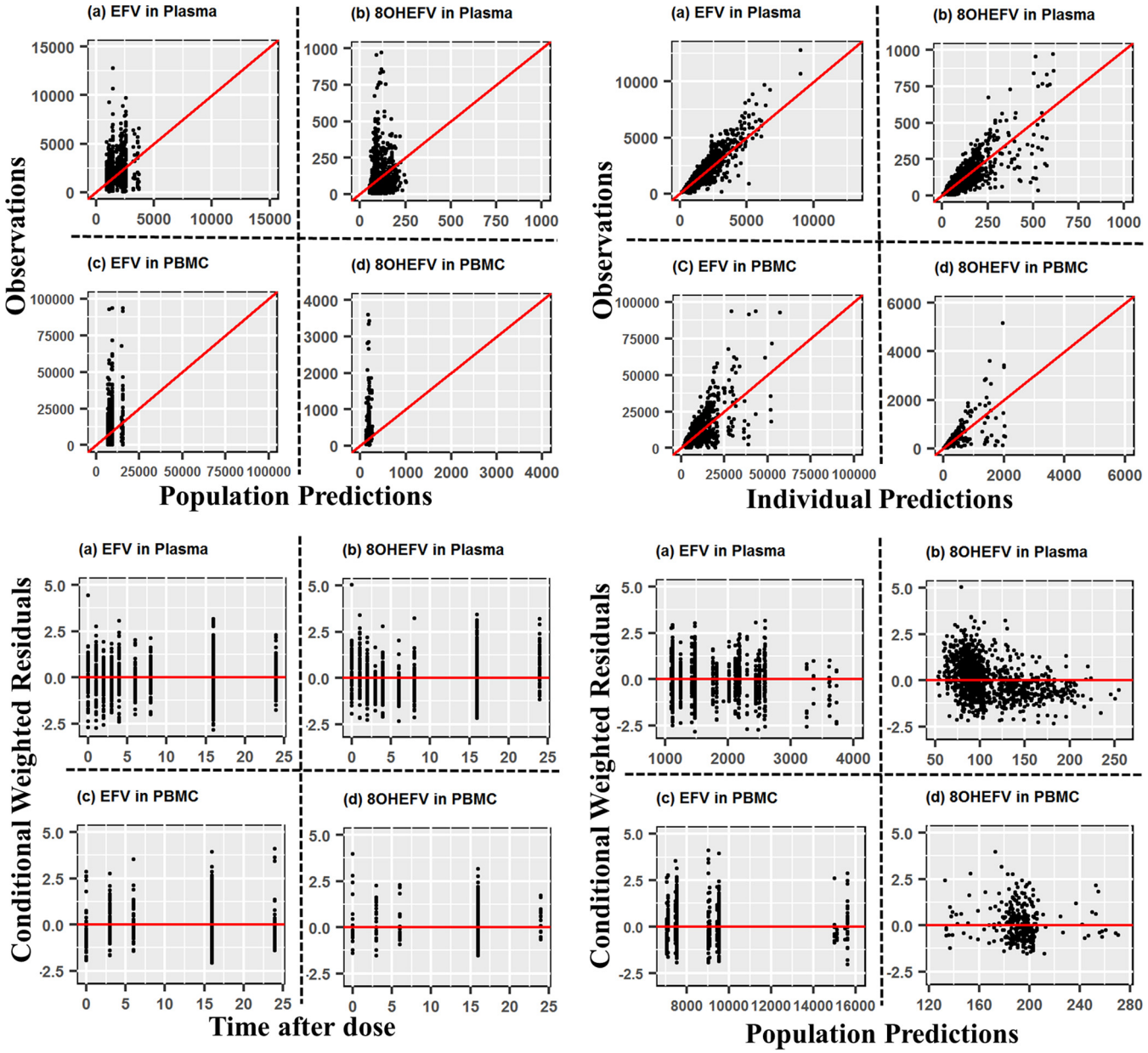

FIG 2 Goodness-of-fit plots of EFV and 8OHEFV in plasma and PBMCs.

(PBMCs), which are the target cells for antiretroviral activity. EFV and 8OHEFV accumulated in greater concentrations intracellularly in PBMCs than in plasma. We also report that the *CYP2B6* genotype was the only covariate that significantly influenced the PK of efavirenz and 8OHEFV.

The efficacy and toxicity of antiretroviral drugs may largely depend on intracellular dispositions in addition to their systemic exposure (16–19). As reviewed by Almond et al., measurement of intracellular concentrations may give a better indication of antiviral exposure as the site of action (20). Besides, Rotger et al. identified intracellular EFV concentration as a predictor of neuropsychological toxicity induced by EFV (21). Efforts to predict safety and efficacy of EFV have focused on characterizing the systemic pharmacokinetics (12, 22, 23). Borand et al. (24) found no association between treatment failure and the recommended efavirenz concentrations in plasma below 1 mg/liter (6). This may suggest that a lack of knowledge of the relationship between plasma and intracellular concentrations of EFV limits the ability to fully understand the

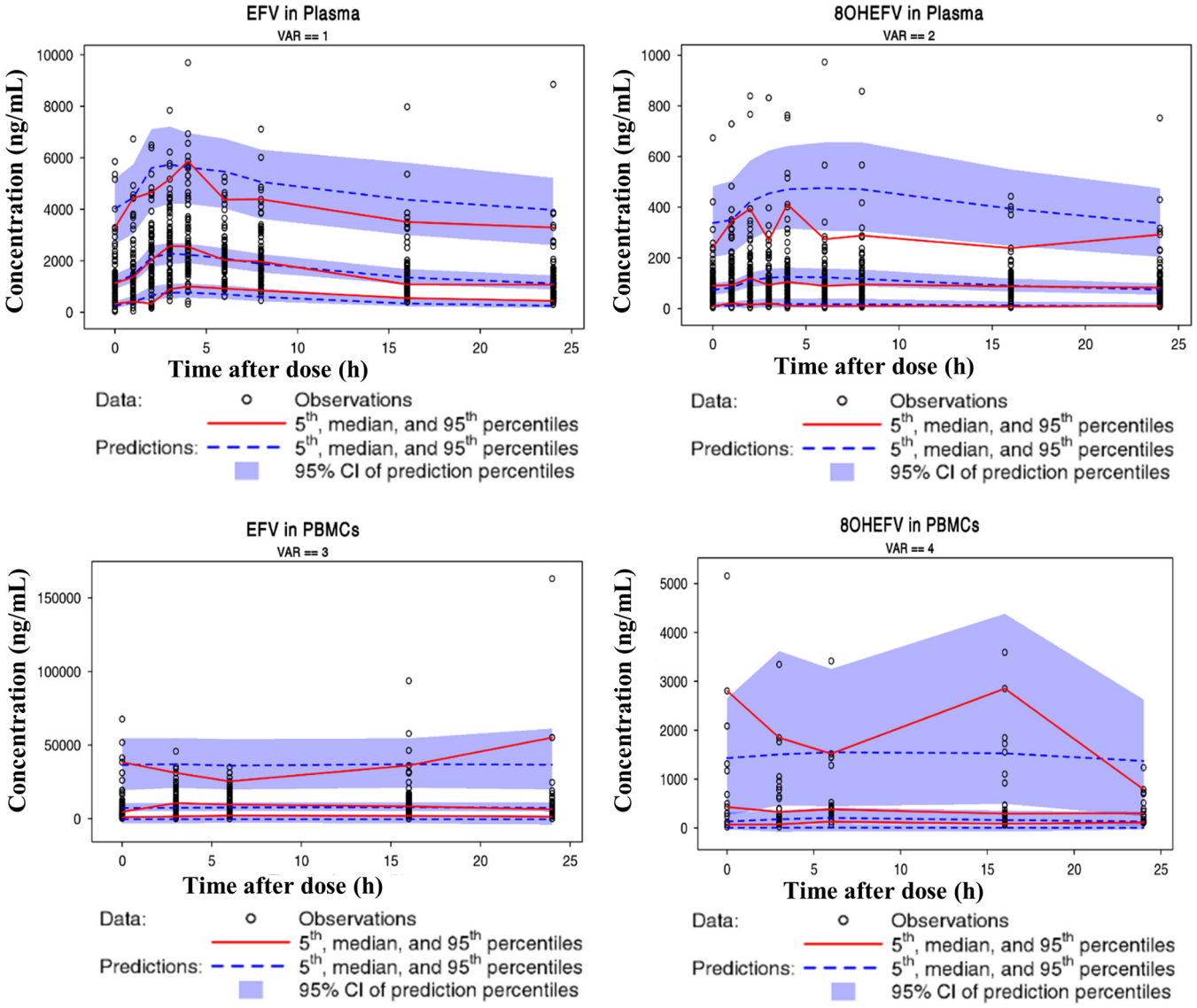

FIG 3 Visual predictive check plots of EFV and 8OHEFV in plasma and PBMCs.

pharmacokinetic-pharmacodynamic relationships of EFV and to predict treatment and toxicity outcomes. A few PK models characterizing other antiretroviral drugs in plasma and the intracellular compartment have been developed (16, 17, 19, 25).

The present study successfully developed a pharmacogenetics-guided comprehensive PK model not only for EFV (the parent drug) but also for 8OHEFV (the major metabolite of EFV) in both plasma and intracellular spaces. The developed model can predict the amount of EFV reaching the site of action and hence may be a useful tool to determine more reliable dosage regimens.

The model shows that the distribution of EFV and 8OHEFV from plasma to PBMCs follows a first-order kinetic process. This suggests that intracellular entry might not involve carrier-mediated transport mechanisms that are saturable in the concentrations observed. This observation may be strengthened by the fact that attempts to investigate whether EFV is a substrate of any of the influx or efflux transport processes have not led to any conclusive outcomes (26, 27). Moreover, in the present study, covariate analysis between the population PK parameters and influx and efflux transporter systems did not reveal any significant impact of the transporters on the PK of EFV and 8OHEFV.

On the contrary, the model shows that the back transfer of EFV and 8OHEFV from PBMCs to plasma follows a Michaelis-Menten kinetics capacity-limited process, a minimized form of a target-mediated drug disposition (TMDD) model. The existence of poor evidence in the involvement of membrane transport mechanisms of EFV as outlined above might suggest the presence of other unidentified processes such as target-mediated binding. Even though the scope of the present study was not to elucidate the mechanistic details, it is assumed that either intracellular protein or tissue binding might limit the back transfer of EFV and 8OHEFV from PBMCs to the plasma compartment. EFV is known to be highly bound to plasma proteins (>99%) and tissue structures (28, 29) and 8OHEFV has been reported to have protein binding similar to that of EFV (30). However, further *in vitro*-supported studies are warranted.

The overall distribution processes of EFV and 8OHEFV from plasma to intracellular spaces and their return kinetics resulted in the net accumulation of EFV and 8OHEFV in PBMCs. This might afford therapeutic advantages or toxicity risks. An increased amount of EFV at the site of action might be utilized to optimize the dose of EFV-based treatment by either lowering the dose or increasing the dosage intervals, which at the end reduces the total exposure of both EFV and 8OHEFV. This might subsequently ensure treatment successes with lower incidences of toxicities from both the parent (EFV) and the metabolite (8OHEFV). Exploration of such regimen changes should be studied only in well controlled clinical trials. Intracellular accumulation of EFV has also been reported by a few investigators. Two independent studies, by Almond et al. (20) and Burhenne et al. (26), showed that EFV accumulation in PBMCs was 1.3- and 1.8-fold higher, respectively, than EFV accumulation in plasma. In the present study, we do not argue that the peripheral compartment is solely represented by PBMCs but rather that it may include other tissues with distribution patterns comparable to those of the PBMCs. Our effort to include a PBMC compartment along with a nonspecific compartment could not be done with the available data.

The *CYP2B6*6* genotype was the only covariate that significantly explained the IIV of EFV clearance. The CL/*F* estimates of EFV for individuals with the *CYP2B6*1/*1*, *CYP2B6*1/*6*, and *CYP2B6*6/*6* genotypes were 18, 14, and 8.6 liters/h, respectively. This finding highlights the growing literature evidence that warrants a pharmacogenetics-based dose adjustment for EFV (3, 5, 22, 31).

The influence of the coadministration of a rifampin (RIF)-based anti-TB regimen on the PK of EFV has been the subject of dispute. Contradictory reports exist in the literature, though recent studies, including our noncompartmental PK and PK-pharmacodynamics (PD) relationship analyses reported on EFV using the same data, suggest the absence of a significant effect of a RIF-based anti-TB regimen (13, 31–33). The covariate analysis in the present study confirmed the absence of the effect of a RIF-based anti-TB regimen on the disposition of EFV and 8OHEFV.

Demographic factors such as age, sex, baseline weight, and body mass index did not improve the goodness-of-fit of the model, implying that they may not explain the observed IIV in the estimated PK parameters of EFV and 8OHEFV. While Dhoro et al. and Robarge et al. identified body weight and sex as covariates to explain the IIV of CL/*F* (3, 34), Abdelhady et al. did not see any influence of demographics on the PK of EFV and metabolites (14). One potential reason for this inconsistency may be differences in study design and PK sampling times. Robarge et al. explored the PK of EFV after a single dose in healthy volunteers, whereas the present study used the steady-state PK of EFV in the target HIV-infected and TB- and HIV-coinfected patient population. We and others have previously demonstrated long-term changes in the PK of EFV due to autoinduction (35). The other reason for the discrepancy might arise from differences in the study population. Previously, we demonstrated differences in the PK of EFV between Ethiopian and Tanzanian HIV patients even after controlling for the effect of the *CYP2B6*6* genotype (36). These inconsistences may indicate not only interindividual but also interpopulation differences in the PK of EFV.

In the present study, even though individual tests of sex and *UGT2B7*2* genotypes on the CL_c/F of 8OHEFV led to significant reductions in OFV ($\alpha = 0.05$), the overall

contributions of these covariates in explaining the IIV of the estimated total clearance of 8OHEFV were small, namely, 2.3% and 0.8%, respectively. These small effects might be assumed to be not clinically significant; therefore, they were not considered true covariates in the final model. The present study also highlighted the absence of an effect of genotype for the influx transporter system OATP1B1 (*1 and *5) and for the efflux transporter ABCB1 (3435C→T and 3842T→C). In addition, baseline liver and renal function tests were not significant determinants of the plasma and intracellular PK parameters of EFV and 8OHEFV.

One limitation of the study was the assumption of 100% adherence to the treatment and time of ingestion of the drug by all patients, which may not reflect the real clinical scenario. Although the investigators tried to capture adherence information in case report forms, these were purely based on self-reports by patients. Similarly, the computation of time-after-dose values for sparse PK samples was based on patient self-reports of the time of ingestion of EFV. The disparity in the time of ingestion to time of sampling was likely minimized (±1 h disparity) through a phone call to each patient reminding them to ingest the daily dose prior to sparse PK sampling next day.

In conclusion, the present study described a population PK model of EFV (parent drug) and 8OHEFV (its major metabolite) in plasma and PBMCs. Both EFV and 8OHEFV followed a first-order transfer process to move from the central to the peripheral compartment, while the reverse transfer was described by a saturable Michaelis-Menten transport process as a simplification of the TMDD model, resulting in a net accumulation of EFV and 8OHEFV in PBMCs. The significance of this finding may suggest a need to explore regimens that lower the dose or increase the dosing interval of EFV, which should only be done in the context of clinical trials. This study also reaffirmed the need for *CYP2B6* genotype-derived dose optimization of EFV. The absence of the influences of demographic factors, RIF-based anti-TB regimen, influx and efflux transport mechanisms, and baseline liver and kidney function tests were highlighted.

MATERIALS AND METHODS

Ethics. The study obtained ethical clearances from Institutional Review Boards, the School of Medicine (Addis Ababa University), and the Karolinska Institutet. In addition, the study protocol obtained approvals from the Addis Ababa Health Bureau, National Research Ethics Review Committee and Drug Administration and Control Authority of Ethiopia. Written informed consent was obtained from all patients to participate in the study. The study was conducted per the international conference for harmonization on good clinical practice recommendations.

Study design and population. This study was a PK substudy of an umbrella study (the HIV-TB Pharmagene study) that was previously described in detail (32, 33). Briefly, the study was an open-label, two-arm, parallel-design, year-long prospective clinical study conducted in a tertiary level referral hospital and eight other health centers in Addis Ababa, Ethiopia. The cohort consisted of HIV-infected patients and TB- and HIV-coinfected patients with CD_4 counts of <200 cells/mm^3. Patients received 600 mg EFV per day as a part of combination antiretroviral therapy (cART). The TB-HIV-coinfected patients were initiated on rifampin-based anti-TB regimens 4 weeks prior to the start of cART. In the present substudy, analyzable PK data from a total of 313 patients, those with HIV infection only ($n = 232$) and those with TB-HIV coinfection ($n = 81$), were included.

PK blood sampling. In the present PK substudy, 19 HIV-only-infected patients and 32 TB-HIV-coinfected patients had week 16 steady-state full concentration-time profiles (0 to 24 h). Plasma samples were collected at 0, 1, 2, 3, 4, 6, 8, 16, and 24 h, and five corresponding PBMC samples were collected at 0, 3, 6, 16, and 24 h. Additionally, the TB-HIV-coinfected patients repeated full-profile sampling 8 weeks after stopping rifampin-based anti-TB drugs at week 32. Two hundred sixty-one patients, who were from either the HIV-only-infected group or the TB-HIV-coinfected group, had 1 or 2 sparse plasma samples with corresponding PBMC samples at 16 ± 1 h postdose at week 4 or week 16 or at both times. Figure 4 shows the PK sampling intervals and study design.

Separation of plasma and PBMC pellets. Isolation of the PBMCs from the plasma was done by centrifugation and subsequent cell counting, as described previously (26, 35). Briefly, 8-ml venous blood samples were collected in BD Vacutainer CPT tubes, in duplicate. To separate the red blood cells from the plasma, the whole-blood samples were centrifuged at 1,700 × *g* for 20 min, within 20 min of collection. The supernatants were decanted in conical tubes, and the tubes containing the supernatant were subjected to centrifugation at 180 × *g* for 10 min to separate the plasma and PBMCs. The plasma specimens were pipetted out into microcentrifuge tubes, and the PBMC pellets were washed two times with 1 ml cold phosphate buffer solution (PBS) and centrifuged again at 180 × *g* at 4°C for 10 min. Finally, the PBMC pellets were resuspended in a 100-μl mixture of 1:10 PBS and trypan blue staining solution,

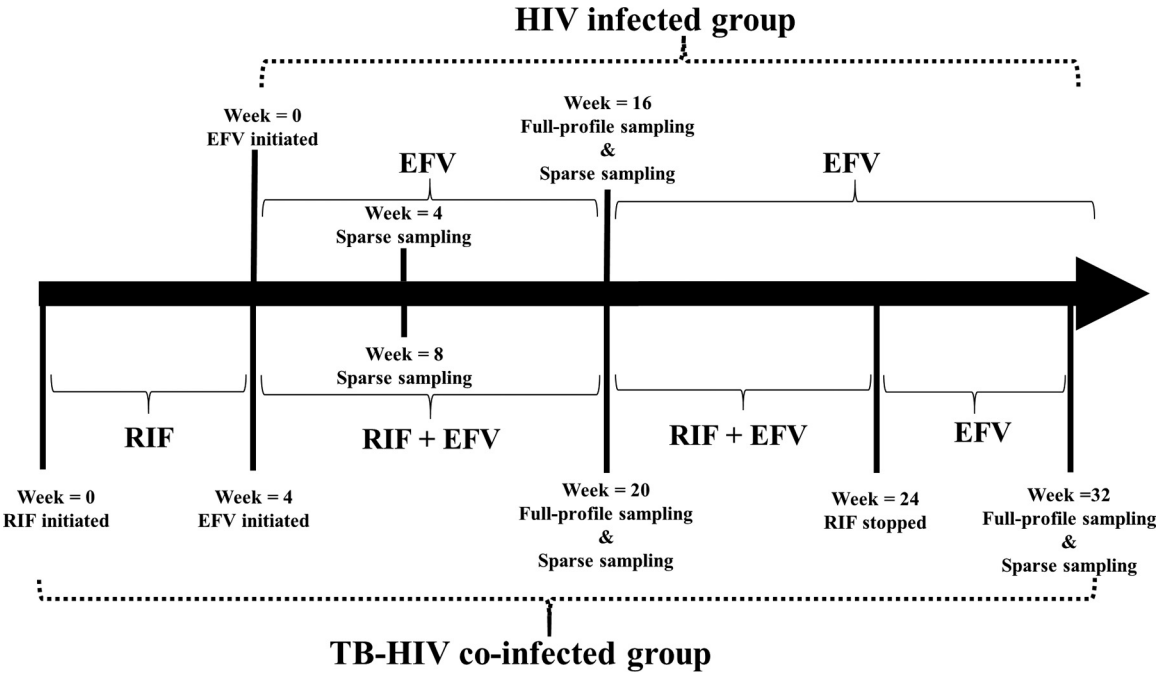

FIG 4 Study design.

and cell counting was performed by trained technicians in Neubauer chambers. The plasma and lysed PBMC pellets were stored at −80°C until bioanalysis.

Bioanalysis of efavirenz and 8-hydroxy-efavirenz. Steady-state plasma and PBMC concentrations of EFV and 8OHEFV were analyzed by liquid chromatography-tandem mass spectrometry (LC-MS/MS), as described previously (35). In brief, protein precipitation with ice-cold acetonitrile containing the internal standards was used for sample preparation and extraction. The extracts containing EFV and 8OHEFV were quantified using [$^{13}C_6$]efavirenz and [$^{2}H_4$]8-hydroxy-efavirenz as internal standards in chromatography on a Phenomenex Synergi Fusion RP column with an eluent consisting of acidified 5 mM ammonium acetate buffer, acetonitrile, and methanol and electrospray tandem mass spectrometry. The lower limits of quantification in plasma were 10 ng/ml for EFV and 0.4 ng/ml for 8OHEFV. The EFV and 8OHEFV calibration ranges were 10 to 10,000 ng/ml and 0.4 to 400 ng/ml, respectively. The plasma and PBMC concentrations of EFV and 8OHEFV above the upper calibration limits were diluted with blank plasma and PBMCs (buffy coat) and reanalyzed. Linear regression with 1/x weighting resulted in correlation coefficients (r^2) of 0.99. The intrabatch and interbatch accuracy and precision of the unknown and quality control concentrations were less than 20%.

Genotype analysis. Genomic DNA was extracted from peripheral blood leukocytes using a QIAamp DNA maxikit (Qiagen GmbH, Hilden, Germany). Single nucleoside polymorphisms (SNPs) of *CYP2B6*6*, *CYP3A5*3*, *CYP3A5*6*, *UGT2B7*2*, *ABCB1* (3435C→T and 3842A→G), *SLCO1B1*1B*, and *SLCO1B1*5* were detected by TaqMan and analyzed using an ABI 7500 system (Applied Biosystems, Foster City, CA, USA) as described previously (33, 37).

Population PK model development. Population PK modeling was performed using the first-order conditional estimation method with eta-epsilon interaction (FOCE-I) in NONMEM version 7.3. Overall, a three-step sequential process for model development was used. First, EFV concentrations in plasma and PBMCs were modeled simultaneously. Subsequently, the empirical Bayesian individual subject parameters of this EFV model were fixed, and concentrations of 8OHEFV in plasma were modeled. Finally, the empirical Bayesian individual subject values of these EFV and 8OHEFV concentrations in plasma parameters were fixed, and concentrations of 8OHEFV in PBMCs were modeled.

Initially, the model building process involved establishment of a base (structural) model by exploring the full concentration-time profile plots of EFV in plasma. The fitting of one-, two-, and three-compartment models with and without absorption lag time (A_{lag}) or transit compartments was applied initially to the full-profile data and subsequently to all EFV plasma and PBMC data. The two-compartment models were fitted by either considering PBMCs as representing the peripheral compartment or as an effect link compartment or with another nonspecified peripheral compartment. The following intercompartmental transfer models were tested in cases of fitting the two-compartment model: first order to and from the central compartment; first order to the peripheral compartment and either zero order or Michaelis-Menten kinetics return to the central compartment. Fitting of three-compartment models was performed by testing either a catenary or mammillary nonspecific compartment while considering PBMCs as a specific peripheral compartment.

Interindividual variability (IIV) in model parameters was modeled as log-normal. Proportional, proportional plus additive, exponential, and additive error models were explored to describe the residual

error. Using only the full-profile plasma concentration-time EFV data, K_a and A_{lag} values were estimated and fixed to these estimates in all subsequent NONMEM runs. With the EFV full-profile model developed, the sparse plasma concentrations were fit together with full-profile plasma data. As strong prior literature suggests that differences in *CYP2B6*6* genotypes are linked to variability in exposure measures of EFV (22, 34, 36–38), *CYP2B6*6* genotype status was included as a modifier of clearance in the base model. Individuals with *CYP2B6*1/*1*, *CYP2B6*1/*6*, and *CYP2B6*6/*6* genotypes were modeled with unique θ (thetas) for EFV clearance.

Compartmental models for EFV and 8OHEFV were parameterized as volumes (V_c EFV, V_p EFV, V_c 8OHEFV, and V_p 8OHEFV) and transfer rate constants (k_{20}, k_{23}, k_{32}, k_{45}, and k_{54}), with derived clearances (CL_c EFV and CL_p EFV are first-order clearance terms for EFV, while CL_c 8OHEFV and CL_p 8OHEFV represent clearances for 8OHEFV from the central to peripheral compartments, respectively). Since the absolute oral bioavailability (F) of EFV cannot be determined in the absence of intravenous administration, the fraction of metabolic conversion of EFV to 8OHEFV also cannot accurately be determined, and clearance and volume of distribution terms for both EFV and 8OHEFV represent apparent values, such as CL/F and V/F. The rate constant terms k_{23} and k_{45} describe first-order transfer processes, while k_{32} and k_{54} represent nonlinear transfer rates defined by the Michaelis-Menten equation (equations 1 and 2). In these equations, V_{max} EFV and V_{max} 8OHEFV represent the maximum rates of transfer of EFV and 8OHEFV, respectively, and K_m EFV and K_m 8OHEFV are concentrations associated with half of the respective V_{max} values. C_{PBMC} EFV and C_{PBMC} 8OHEFV represent the concentrations of EFV and 8OHEFV in PBMCs, respectively.

$$K_{32} = \frac{V_{max}\ \mathrm{EFV}}{K_m\ \mathrm{EFV} + C_{PBMC}\ \mathrm{EFV}} \times \frac{1}{V_p\ \mathrm{EFV}} \quad (1)$$

$$K_{54} = \frac{V_{max}\ \mathrm{8OHEFV}}{K_m\ \mathrm{8OHEFV} + C_{PBMC}\ \mathrm{8OHEFV}} \times \frac{1}{V_p\ \mathrm{8OHEFV}} \quad (2)$$

Covariate relationships in EFV CL_c/F, V_c/F, and V_{max} as well as in 8OHEFV CL_c/F were explored first using delta plots, where the delta plot represents the difference between the individual and typical parameter values on the y axis versus the covariate values on the x axis. Where trends were observed, a stepwise forward addition of covariates ($\alpha = 0.05$) with a backward elimination ($\alpha = 0.01$) was performed. The covariates explored were demographic characteristics (baseline body weight, sex, age, and body mass index), baseline liver function tests (alanine aminotransferase [ALT], aspartate aminotransferase [AST], alkaline phosphatase [ALP]), baseline renal function tests (serum creatinine and blood urea), rifampin-based anti-TB comedication, and the pharmacogenetic variables *CYP3A5*3*, *CYP3A5*6*, *UGT2B7*2*, *ABCB1* (3435 C→T and 3842 T→C), *OATP1B1*1B*, and *OATP1B1*5*.

Subsequent to the development of the EFV model, the 8OHEFV concentrations in plasma were modeled, and empirical Bayesian estimates of the individual subject EFV PK parameters were fixed in the model of the 8OHEFV concentrations in plasma. A 77% conversion of EFV to 8OHEFV was assumed (39). Finally, 8OHEFV concentrations in PBMCs were modeled by fixing the individual PK parameter estimates of EFV in plasma and PBMCs as well as 8OHEFV in plasma. Since TB-HIV-coinfected patients had participated in the PK sampling on two occasions, the influence of interoccasion variability (IOV) on clearances of both EFV and 8OHEFV was also tested.

Model diagnostics and evaluations. Model diagnostics were performed and evaluated by graphical and statistical methods. Graphical diagnostics and evaluation plots were generated using KIWI version 1.6 (Simulations Plus, Inc.). Comparisons of the minimum objective function value (OFV) were used to discriminate between competing models. A decrease of 3.84 in OFV was related to a statistically significant improvement between models ($\alpha = 0.05$, χ^2 distribution). Parameter standard errors of the mean (%SEM) and coefficients of variation (%CV) were obtained using the covariance option ($COV) of NONMEM.

The comprehensive final model describing the time course of EFV and 8OHEFV in plasma and PBMCs was evaluated by its predictive performance. Visual predictive check (VPC) was performed by simulating 1,000 replicates based on the final model parameters and examining the agreement between model-based simulations and observed data with 5th and 95th percentile confidence intervals.

ACKNOWLEDGMENTS

We express our gratitude to all the study participants and to the staff who conducted the study.

This work was supported by research grants from the European and Developing Countries Clinical Trial Partnership (grant CT.2005.32030.001), the Swedish International Development Agency (grants HIV-2006-031 and SWE 2007–270), and the Swedish Research Council (grant 348-2011-7383).

We declare no conflicts of interest.

A.H., E.A., E.M., G.Y., L.B., J.B., and J.S.O. conceived and designed the experiments, A.H., E.A., J.B., and J.S.O. performed the experiments, A.H., E.A., J.B., and J.S.O. analyzed the data, A.H., E.A., E.M., G.Y., L.B., J.B., and J.S.O. contributed reagents, materials, and analysis tools, and A.H., E.A., J.B., and J.S.O. wrote the paper. All authors read and approved the final manuscript.

REFERENCES

1. WHO. 2016. Consolidated guidelines on the use of antiretroviral drugs for treating and preventing HIV infection: recommendations for a public health approach. World Health Organization, Geneva, Switzerland. http://www.who.int/hiv/pub/arv/arv-2016/en/.
2. Gunda DW, Kasang C, Kidenya BR, Kabangila R, Mshana SE, Kidola J, Kalluvya SE, Kongola GW, Klinker H. 2013. Plasma concentrations of efavirenz and nevirapine among HIV-infected patients with immunological failure attending a tertiary hospital in North-western Tanzania. PLoS One 8:e75118. https://doi.org/10.1371/journal.pone.0075118.
3. Robarge JD, Metzger IF, Lu J, Thong N, Skaar TC, Desta Z, Bies RR. 2017. Population pharmacokinetic modeling to estimate the contribution of genetic and nongenetic factors of efavirenz disposition. Antimicrob Agents Chemother 61:e01813-16. https://doi.org/10.1128/AAC.01813-16.
4. Calcagno A, Cusato J, D'Avolio A, Bonora S. 2017. Genetic polymorphisms affecting the pharmacokinetics of antiretroviral drugs. Clin Pharmacokinet 56:355–369. https://doi.org/10.1007/s40262-016-0456-6.
5. Gengiah TN, Botha JH, Yende-Zuma N, Naidoo K, Abdool Karim SS. 2015. Efavirenz dosing: influence of drug metabolizing enzyme polymorphisms and concurrent tuberculosis treatment. Antivir Ther 20:297–306. https://doi.org/10.3851/IMP2877.
6. Manosuthi W, Sungkanuparph S, Thakkinstian A, Vibhagool A, Kiertiburanakul S, Rattanasiri S, Prasithsirikul W, Sankote J, Mahanontharit A, Ruxrungtham K. 2005. Efavirenz levels and 24-week efficacy in HIV-infected patients with tuberculosis receiving highly active antiretroviral therapy and rifampicin. AIDS 19:1481–1486. https://doi.org/10.1097/01.aids.0000183630.27665.30.
7. Arend C, Rother A, Stolte S, Dringen R. 2016. Consequences of a chronic exposure of cultured brain astrocytes to the anti-retroviral drug efavirenz and its primary metabolite 8-hydroxy efavirenz. Neurochem Res 41:3278–3288. https://doi.org/10.1007/s11064-016-2059-x.
8. Mukonzo JK, Nanzigu S, Rekic D, Waako P, Roshammar D, Ashton M, Ogwal-Okeng J, Gustafsson LL, Aklillu E. 2011. HIV/AIDS patients display lower relative bioavailability of efavirenz than healthy subjects. Clin Pharmacokinet 50:531–540. https://doi.org/10.2165/11592660-000000000-00000.
9. Tovar-y-Romo LB, Bumpus NN, Pomerantz D, Avery LB, Sacktor N, McArthur JC, Haughey NJ. 2012. Dendritic spine injury induced by the 8-hydroxy metabolite of efavirenz. J Pharmacol Exp Ther 343:696–703. https://doi.org/10.1124/jpet.112.195701.
10. Csajka C, Marzolini C, Fattinger K, Decosterd LA, Fellay J, Telenti A, Biollaz J, Buclin T. 2003. Population pharmacokinetics and effects of efavirenz in patients with human immunodeficiency virus infection. Clin Pharmacol Ther 73:20–30. https://doi.org/10.1067/mcp.2003.22.
11. Ke A, Barter Z, Rowland-Yeo K, Almond L. 2016. Towards a best practice approach in PBPK modeling: case example of developing a unified efavirenz model accounting for induction of CYPs 3A4 and 2B6. CPT Pharmacometrics Syst Pharmacol 5:367–376. https://doi.org/10.1002/psp4.12088.
12. Luo M, Chapel S, Sevinsky H, Savant I, Cirincione B, Bertz R, Roy A. 2016. Population pharmacokinetics analysis to inform efavirenz dosing recommendations in pediatric HIV patients aged 3 months to 3 years. Antimicrob Agents Chemother 60:3676–3686. https://doi.org/10.1128/AAC.02678-15.
13. Mukonzo JK, Nanzigu S, Waako P, Ogwal-Okeng J, Gustafson LL, Aklillu E. 2014. CYP2B6 genotype, but not rifampicin-based anti-TB cotreatments, explains variability in long-term efavirenz plasma exposure. Pharmacogenomics 15:1423–1435. https://doi.org/10.2217/pgs.14.73.
14. Abdelhady AM, Desta Z, Jiang F, Yeo CW, Shin JG, Overholser BR. 2014. Population pharmacogenetic-based pharmacokinetic modeling of efavirenz, 7-hydroxy- and 8-hydroxyefavirenz. J Clin Pharmacol 54:87–96. https://doi.org/10.1002/jcph.208.
15. Minuesa G, Huber-Ruano I, Pastor-Anglada M, Koepsell H, Clotet B, Martinez-Picado J. 2011. Drug uptake transporters in antiretroviral therapy. Pharmacol Ther 132:268–279. https://doi.org/10.1016/j.pharmthera.2011.06.007.
16. Chen X, Seifert SM, Castillo-Mancilla JR, Bushman LR, Zheng JH, Kiser JJ, MaWhinney S, Anderson PL. 2016. Model linking plasma and intracellular tenofovir/emtricitabine with deoxynucleoside triphosphates. PLoS One 11:e0165505. https://doi.org/10.1371/journal.pone.0165505.
17. Seifert SM, Chen X, Meditz AL, Castillo-Mancilla JR, Gardner EM, Predhomme JA, Clayton C, Austin G, Palmer BE, Zheng JH, Klein B, Kerr BJ, Guida LA, Rower C, Rower JE, Kiser JJ, Bushman LR, MaWhinney S, Anderson PL. 2016. Intracellular tenofovir and emtricitabine anabolites in genital, rectal, and blood compartments from first dose to steady state. AIDS Res Hum Retroviruses 32:981–991. https://doi.org/10.1089/aid.2016.0008.
18. Wang L, Soon GH, Seng KY, Li J, Lee E, Yong EL, Goh BC, Flexner C, Lee L. 2011. Pharmacokinetic modeling of plasma and intracellular concentrations of raltegravir in healthy volunteers. Antimicrob Agents Chemother 55:4090–4095. https://doi.org/10.1128/AAC.00593-11.
19. Zhou Z, Rodman JH, Flynn PM, Robbins BL, Wilcox CK, D'Argenio DZ. 2006. Model for intracellular lamivudine metabolism in peripheral blood mononuclear cells ex vivo and in human immunodeficiency virus type 1-infected adolescents. Antimicrob Agents Chemother 50:2686–2694. https://doi.org/10.1128/AAC.01637-05.
20. Almond LM, Hoggard PG, Edirisinghe D, Khoo SH, Back DJ. 2005. Intracellular and plasma pharmacokinetics of efavirenz in HIV-infected individuals. J Antimicrob Chemother 56:738–744. https://doi.org/10.1093/jac/dki308.
21. Rotger M, Colombo S, Furrer H, Bleiber G, Buclin T, Lee BL, Keiser O, Biollaz J, Decosterd L, Telenti A, Swiss HIVCS. 2005. Influence of CYP2B6 polymorphism on plasma and intracellular concentrations and toxicity of efavirenz and nevirapine in HIV-infected patients. Pharmacogenet Genomics 15:1–5. https://doi.org/10.1097/01213011-200501000-00001.
22. Hui KH, Lee SS, Lam TN. 2016. Dose optimization of efavirenz based on individual CYP2B6 polymorphisms in Chinese patients positive for HIV. CPT Pharmacometrics Syst Pharmacol 5:182–191. https://doi.org/10.1002/psp4.12067.
23. Mukonzo JK, Owen JS, Ogwal-Okeng J, Kuteesa RB, Nanzigu S, Sewankambo N, Thabane L, Gustafsson LL, Ross C, Aklillu E. 2014. Pharmacogenetic-based efavirenz dose modification: suggestions for an African population and the different CYP2B6 genotypes. PLoS One 9:e86919. https://doi.org/10.1371/journal.pone.0086919.
24. Borand L, Madec Y, Laureillard D, Chou M, Marcy O, Pheng P, Prak N, Kim C, Lak KK, Hak C, Dim B, Nerrienet E, Fontanet A, Sok T, Goldfeld AE, Blanc FX, Taburet AM. 2014. Plasma concentrations, efficacy and safety of efavirenz in HIV-infected adults treated for tuberculosis in Cambodia (ANRS 1295-CIPRA KH001 CAMELIA trial). PLoS One 9:e90350. https://doi.org/10.1371/journal.pone.0090350.
25. Baheti G, Kiser JJ, Havens PL, Fletcher CV. 2011. Plasma and intracellular population pharmacokinetic analysis of tenofovir in HIV-1-infected patients. Antimicrob Agents Chemother 55:5294–5299. https://doi.org/10.1128/AAC.05317-11.
26. Burhenne J, Matthee AK, Pasakova I, Roder C, Heinrich T, Haefeli WE, Mikus G, Weiss J. 2010. No evidence for induction of ABC transporters in peripheral blood mononuclear cells in humans after 14 days of efavirenz treatment. Antimicrob Agents Chemother 54:4185–4191. https://doi.org/10.1128/AAC.00283-10.
27. Mukonzo JK, Roshammar D, Waako P, Andersson M, Fukasawa T, Milani L, Svensson JO, Ogwal-Okeng J, Gustafsson LL, Aklillu E. 2009. A novel polymorphism in ABCB1 gene, CYP2B6*6 and sex predict single-dose efavirenz population pharmacokinetics in Ugandans. Br J Clin Pharmacol 68:690–699. https://doi.org/10.1111/j.1365-2125.2009.03516.x.
28. Boffito M, Back DJ, Blaschke TF, Rowland M, Bertz RJ, Gerber JG, Miller V. 2003. Protein binding in antiretroviral therapies. AIDS Res Hum Retroviruses 19:825–835. https://doi.org/10.1089/088922203769232629.
29. Sikora MJ, Rae JM, Johnson MD, Desta Z. 2010. Efavirenz directly modulates the oestrogen receptor and induces breast cancer cell growth. HIV Med 11:603–607. https://doi.org/10.1111/j.1468-1293.2010.00831.x.
30. Avery LB, VanAusdall JL, Hendrix CW, Bumpus NN. 2013. Compartmentalization and antiviral effect of efavirenz metabolites in blood plasma, seminal plasma, and cerebrospinal fluid. Drug Metab Dispos 41:422–429. https://doi.org/10.1124/dmd.112.049601.
31. Mukonzo JK, Bisaso RK, Ogwal-Okeng J, Gustafsson LL, Owen JS, Aklillu E. 2016. CYP2B6 genotype-based efavirenz dose recommendations during rifampicin-based antituberculosis cotreatment for a sub-Saharan Africa population. Pharmacogenomics 17:603–613. https://doi.org/10.2217/pgs.16.7.
32. Habtewold A, Aklillu E, Makonnen E, Amogne W, Yimer G, Aderaye G, Bertilsson L, Owen JS, Burhenne J. 2016. Long-term effect of rifampicin-based anti-TB regimen coadministration on the pharmacokinetic param-

eters of efavirenz and 8-hydroxy-efavirenz in Ethiopian patients. J Clin Pharmacol 56:1538–1549. https://doi.org/10.1002/jcph.756.
33. Habtewold A, Makonnen E, Amogne W, Yimer G, Aderaye G, Bertilsson L, Burhenne J, Aklillu E. 2015. Is there a need to increase the dose of efavirenz during concomitant rifampicin-based antituberculosis therapy in sub-Saharan Africa? The HIV-TB Pharmagene Study. Pharmacogenomics 16:1047–1064. https://doi.org/10.2217/pgs.15.35.
34. Dhoro M, Zvada S, Ngara B, Nhachi C, Kadzirange G, Chonzi P, Masimirembwa C. 2015. CYP2B6*6, CYP2B6*18, body weight and sex are predictors of efavirenz pharmacokinetics and treatment response: population pharmacokinetic modeling in an HIV/AIDS and TB cohort in Zimbabwe. BMC Pharmacol Toxicol 16:4. https://doi.org/10.1186/s40360-015-0004-2.
35. Habtewold A, Amogne W, Makonnen E, Yimer G, Riedel KD, Ueda N, Worku A, Haefeli WE, Lindquist L, Aderaye G, Burhenne J, Aklillu E. 2011. Long-term effect of efavirenz autoinduction on plasma/peripheral blood mononuclear cell drug exposure and CD4 count is influenced by UGT2B7 and CYP2B6 genotypes among HIV patients. J Antimicrob Chemother 66:2350–2361. https://doi.org/10.1093/jac/dkr304.
36. Ngaimisi E, Mugusi S, Minzi O, Sasi P, Riedel KD, Suda A, Ueda N, Janabi M, Mugusi F, Haefeli WE, Bertilsson L, Burhenne J, Aklillu E. 2011. Effect of rifampicin and CYP2B6 genotype on long-term efavirenz autoinduction and plasma exposure in HIV patients with or without tuberculosis. Clin Pharmacol Ther 90:406–413. https://doi.org/10.1038/clpt.2011.129.
37. Ngaimisi E, Habtewold A, Minzi O, Makonnen E, Mugusi S, Amogne W, Yimer G, Riedel KD, Janabi M, Aderaye G, Mugusi F, Bertilsson L, Aklillu E, Burhenne J. 2013. Importance of ethnicity, CYP2B6 and ABCB1 genotype for efavirenz pharmacokinetics and treatment outcomes: a parallel-group prospective cohort study in two sub-Saharan Africa populations. PLoS One 8:e67946. https://doi.org/10.1371/journal.pone.0067946.
38. Colic A, Alessandrini M, Pepper MS. 2015. Pharmacogenetics of CYP2B6, CYP2A6 and UGT2B7 in HIV treatment in African populations: focus on efavirenz and nevirapine. Drug Metab Rev 47:111–123. https://doi.org/10.3109/03602532.2014.982864.
39. Ogburn ET, Jones DR, Masters AR, Xu C, Guo Y, Desta Z. 2010. Efavirenz primary and secondary metabolism in vitro and in vivo: identification of novel metabolic pathways and cytochrome P450 2A6 as the principal catalyst of efavirenz 7-hydroxylation. Drug Metab Dispos 38:1218–1229. https://doi.org/10.1124/dmd.109.031393.